

GScomp-QA: A Subjective Dataset for Quality Assessment of Compressed Gaussian Splatting

Pedro Martin

Instituto Superior Técnico
Instituto Telecomunicações
Lisbon, Portugal
pedro.martin@lx.it.pt

António Rodrigues

Instituto Superior Técnico
Instituto Telecomunicações
Lisbon, Portugal
antonio.rodrigues@lx.it.pt

João Ascenso

Instituto Superior Técnico
Instituto Telecomunicações
Lisbon, Portugal
joao.ascenso@lx.it.pt

Maria Paula Queluz

Instituto Superior Técnico
Instituto Telecomunicações
Lisbon, Portugal
paula.queluz@lx.it.pt

ABSTRACT

Gaussian Splatting (GS) has emerged as an efficient representation for high-quality 3D reconstruction and novel view synthesis. However, its large model size poses challenges for storage and transmission. While several GS compression solutions have been proposed, their perceptual impact remains poorly understood due to the lack of dedicated evaluation datasets. To address this gap, this paper introduces GScomp-QA, a subjective quality assessment dataset for evaluating synthesis quality from compressed GS models. The dataset comprises 331 video stimuli from 13 real-world scenes, covering 9 state-of-the-art GS compression solutions. By using videos synthesized from uncompressed models as reference, GScomp-QA isolates compression-induced distortions from synthesis artifacts. A subjective study with 20 participants was conducted, providing reliable perceptual scores. Based on these data, GS compression solutions are evaluated through perceptual rate-distortion analysis. In addition, 18 objective quality metrics are evaluated, showing that they do not fully capture GS-specific distortions. GScomp-QA will be publicly available and provide a benchmark for evaluating GS compression solutions and supporting the development of quality metrics tailored to GS compression.

CCS CONCEPTS

- Information systems → Multimedia content creation;
- Computing methodologies → Volumetric compression.

KEYWORDS

Dataset, Gaussian Splatting, Compression, Quality Assessment, Benchmark, View Synthesis

1 Introduction

The demand for immersive 3D visual experiences has grown significantly in recent years [1]. Applications such as virtual reality, augmented reality, telepresence, and digital heritage require scene representations that provide high-quality rendering from arbitrary viewpoints while maintaining real-time performance. Gaussian Splatting (GS) [2] has recently emerged as a promising paradigm for novel view synthesis, representing scenes as collections of 3D Gaussians parameterized by spatial attributes and view-dependent appearance.

Despite its advantages, GS models may reach gigabyte-scale sizes due to the large number of Gaussians and their high-dimensional parameterization. This poses major challenges for storage and transmission, making compression critical for practical deployment. However, assessing the perceptual impact of GS compression is challenging, as compression artifacts are entangled with distortions inherent to the view synthesis process. Existing studies often fail to isolate these effects, making it difficult to assess the perceptual impact of compression. Furthermore, the scarcity of publicly available perceptual datasets for compressed GS hinders both the design of dedicated quality metrics and the benchmarking of compression solutions.

To address these limitations, this paper introduces GScomp-QA, a subjective quality assessment dataset for compressed GS view synthesis, aiming to provide a deeper understanding of the perceptual impact of GS compression. The dataset supports three key use cases: (i) developing perceptually grounded objective quality metrics suitable for GS codec optimization and evaluation; (ii) benchmarking state-of-the-art GS compression solutions; and (iii) validating existing and future quality metrics for compressed GS models. The main contributions of this work are as follows:

- **Perceptual dataset for compressed GS view synthesis:** GScomp-QA comprises synthesized videos and their associated subjective scores, obtained from a subjective assessment of several state-of-the-art GS compression solutions across diverse scenes. By using videos synthesized from uncompressed GS models as reference, compression-induced degradations are isolated from synthesis artifacts. It provides a benchmark for perceptually aware GS compression and the development of compression-specific quality metrics.
- **Benchmarking of GS compression solutions:** A comparative study of state-of-the-art GS compression strategies is conducted across several scenes and quality levels, providing

[†]Author Footnote to be captured as Author Note

Permission to make digital or hard copies of part or all of this work for personal or classroom use is granted without fee provided that copies are not made or distributed for profit or commercial advantage and that copies bear this notice and the full citation on the first page. Copyrights for third-party components of this work must be honored. For all other uses, contact the owner/author(s).

WOODSTOCK '18, June, 2018, El Paso, Texas USA

© 2018 Copyright held by the owner/author(s). 978-1-4503-0000-0/2005/06
<https://doi.org/10.1145/1234567890>

insights into model-dependent behaviors and perceptual rate-quality trade-offs.

- **Objective quality metrics evaluation:** A comprehensive evaluation of existing objective quality metrics is conducted against the subjective scores of GScomp-QA, assessing their reliability and suitability for predicting the perceptual impact of GS compression.

The rest of this paper is organized as follows: Section 2 reviews related work. Section 3 describes the GScomp-QA dataset generation framework. Section 4 presents the subjective assessment design. Section 5 analyses the subjective tests results and benchmarks the performance of GS compression solutions. Section 6 evaluates the performance of quality metrics on the proposed dataset. Section 7 concludes the paper. The dataset is publicly available at [3] under a CC BY-SA 4.0 license. Supplementary material is provided on the dataset webpage.

2 Related Work

Quality assessment of GS-generated content has received growing attention in recent years. GS-QA [4] introduced the first subjective dataset evaluating GS view synthesis quality across multiple GS methods and real-world scenes. However, it does not investigate the perceptual impact of GS model compression.

3DGS-IEval-15K [5] is an image dataset specifically designed for compressed GS models under varying viewpoints. While valuable, it does not fully reflect practical scenarios, where novel view synthesis is typically experienced as a continuous visual stream through smooth camera motion or interactive exploration. Temporal artifacts such as flickering, geometric instability, and view-dependent inconsistencies are often perceptible only during viewpoint transitions, making them difficult to capture through isolated image evaluation. Furthermore, this dataset is not currently publicly available.

3DGS-VBench [6] evaluates compressed GS models using synthesized videos but is not publicly accessible at the time of writing. Furthermore, it adopts a categorical rating methodology without an explicit reference sequence, making it unable to isolate the perceptual quality impact of compression from view synthesis artifacts.

Other GS quality assessment datasets only partially address compression-related distortions. Datasets such as 3DGS-QA [7] and MUGSQA [8] focus on distortions arising from factors such as number of training images, number of training iterations, noise presence, or downsampling, rather than artifacts introduced by dedicated GS compression solutions. Moreover, 3DGS-QA and MUGSQA are limited to synthetic scenes, which lack the structural complexity and perceptual richness of real-world captures. GSCQA [9] includes compressed GS content, but its scope is limited to the artifacts produced by their proposed compression pipeline, without considering alternative GS compression solutions.

The GScomp-QA dataset proposed in this work addresses these limitations along several dimensions. First, subjects evaluate synthesized videos rather than isolated images, enabling the assessment of temporal and view-dependent artifacts. Second, subjective quality is measured using the uncompressed GS

representation as reference, allowing compression effects to be studied independently of synthesis artifacts. Third, it covers two baseline GS representations paired with several compression solutions, ensuring diverse compression-induced distortions and finally, the dataset includes real-world scenes, preserving the richness and complexity of natural content. Together, these design choices make GScomp-QA a comprehensive benchmark for GS compression evaluation and objective quality metric development and validation.

3 GScomp-QA Dataset Design

This section describes the framework used to create the proposed dataset, comprising the stimuli and the associated subjective scores. Section 3.1 presents the overall pipeline, Section 3.2 describes the selected GS compression solutions, and Section 3.3 presents the selected visual scenes.

3.1 Framework Overview

The GScomp-QA framework takes as input a set of captured images, with the respective camera poses and the point cloud (PC) generated by a structure-from-motion algorithm [10, 11], and produces the test and reference sequences for several GS compression solutions and associated quality scores. As depicted in Figure 1, the framework has two parallel branches: the reference branch (top) synthesizes video from an uncompressed (baseline) GS model, while the test branch (bottom) synthesizes video from a compressed GS model. The uncompressed baseline serves as reference, instead of the original captured content, allowing compression-induced distortions to be assessed independently of view synthesis artifacts. The GScomp-QA dataset comprises the synthesized videos and their associated subjective scores (red box in Figure 1), generated through the following stages:

GS Training. A baseline GS model is trained using the input images, PC, and camera poses (green box in Figure 1). Two GS baselines are considered: 3DGS [2], which represents Gaussian parameters explicitly, and Scaffold-GS [12], which encodes them implicitly through voxel-grid features and MLPs, thus offering two fundamentally different scene representations. Existing GS compression solutions are typically designed for one of these two representations. In 3DGS, each Gaussian is independently defined by explicit parameters including position, covariance (parameterized by scale and rotation), opacity, and view-dependent color. Scaffold-GS instead anchors the representation on a sparse voxel grid, where local Gaussian attributes are predicted from anchor features using MLPs. The training process optimizes the model parameters end-to-end by minimizing a reconstruction loss between synthesized and ground-truth training views, rendered through a differentiable tile-based rasterizer.

GS Training plus Compression. Depending on the strategy, GS compression may be coupled with the training process (model creation) or applied as a post-training stage. In both cases, the GS model parameters are encoded into a compact bitstream and this encoding is typically lossy. Section 3.2 details the selected compression approaches.

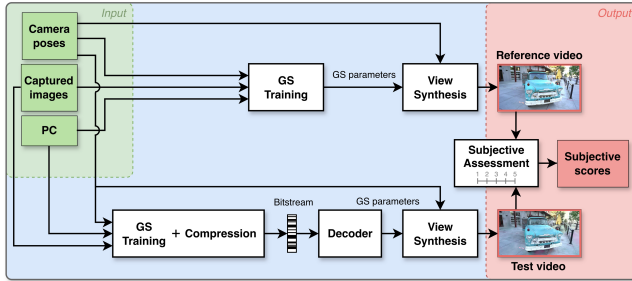


Figure 1: GScomp-QA framework.

Decoder. The bitstream is decoded to reconstruct the GS parameters, which are then used for view synthesis. The decoder mirrors the inverse operations of the encoding process, recovering the GS model.

View Synthesis. Novel views are synthesized from both the compressed and uncompressed GS models, producing the test and reference videos, respectively. For each input scene, all videos are synthesized using an identical camera trajectory to ensure a valid comparison. The trajectory is derived from the training camera poses, following the approach of [13]: a focal point is estimated as the point that minimizes the sum of squared distances to all training camera optical axes; an elliptical orbit is then fitted around this focal point, with semi-axes set to the 90th percentile of the training camera position deviations along each spatial dimension. A 10 s video with 24 fps is then synthesized along this trajectory.

Subjective Assessment. The resulting video pairs are evaluated with a semi-controlled subjective assessment experiment, described in Section 4.2. Note that the reference video of the pair is synthesized from an uncompressed baseline GS model (either 3DGS or Scaffold-GS), while each test video of the pair is synthesized from a compressed model produced by a codec designed for that baseline representation.

3.2 Selected GS Compression Solutions

This section presents the GS compression solutions selected for the creation of the dataset, broadly categorized into two classes based on their interaction with the training process.

3.2.1 Joint Training and Compression. These methods integrate compression constraints directly into the GS training process, jointly optimizing for both reconstruction quality and model compactness. For 3DGS-based representations, Reduced3DGS [14] and Compact3D [15] progressively prune redundant Gaussians during training and apply vector quantization to the parameters of the retained Gaussians. For Scaffold-GS-based representations, HAC++ [16] exploits the relationship between unorganized anchors and a structured hash grid, using their mutual information for context modeling, combined with intra-anchor redundancy reduction. ContextGS [17] introduces an autoregressive context model that organizes anchors into hierarchical levels, where already coded anchors at coarser levels are used to predict finer-level anchors, improving entropy coding efficiency. Joint training and compression solutions generally achieve high rate-distortion (RD) performances, as the model

learning is explicitly optimized for compression. However, since the compression is tightly coupled with the training process, these methods require access to the original input data to compress a GS model, which is rarely available in real-world scenarios.

3.2.2 Post-Training Compression. These methods compress pre-trained GS models directly. For 3DGS-based representations, GSICO-3DGS [18] maps Gaussian parameters onto structured 2D images through a spatially coherent arrangement algorithm, enabling their compression with a conventional image codec; FCGS [19] employs a learned feed-forward compression model with context modeling, enabling compression of any pre-trained model in a single pass without per-scene optimization. For Scaffold-GS-based methods, GSICO-Scaffold-GS [18] extends the image-based coding approach to the voxel-based representation of Scaffold-GS, and is, to the best of the authors' knowledge, the only post-training compression solution specifically designed for this representation. Although primarily a post-training codec, SOG [20] also modifies the GS training process itself to organize Gaussian parameters into a locally smooth 2D grid, making the resulting model more amenable to compression. Thus, SOG occupies an intermediate position between joint training and compression and purely post-training approaches. Other methods such as LightGaussian [21] introduce a fine-tuning phase to recover quality lost during the compression process (made of pruning and vector quantization operations).

3.3 Selected Visual Scenes

The GScomp-QA dataset is built upon visual scenes drawn from publicly available datasets widely used in GS research [1], selected to ensure diversity in scene structure, scale, and capture conditions: Tanks and Temples (T&T) [22], with *train* and *truck* scenes; Deep Blending (DB) [23], with *drjohnson* and *playroom*; Light Field (LF) [24], with *africa*, *basket*, and *ship*; and MipNeRF360 (M360) [25], with *bicycle*, *bonsai*, *counter*, *flowers*, *garden*, and *kitchen*; resulting in a total of 13 visual scenes.

These are static scenes that span a wide variety of characteristics. In terms of environment, all scenes from T&T and *bicycle*, *flowers*, and *garden* scenes from M360, are outdoor scenes, while all scenes from DB, LF, and the scenes *bonsai*, *counter*, and *kitchen* from M360, are indoor scenes. Regarding camera capturing style, T&T, LF, and M360 use a 360° trajectory, and DB uses a freestyle acquisition. The selected scenes also differ in spatial extent, ranging from small-scale indoor environments to large-scale outdoor settings. Table 1 specifies the number of training images and spatial resolution of each scene.

4 Subjective Test Design and Procedure

This section describes the subjective test design and procedure used to generate the GScomp-QA dataset. Section 4.1 presents the test conditions, Section 4.2 details the subjective methodology, and Section 4.3 describes the data processing applied to derive the final subjective scores, including a reference compensation procedure used to enable the comparison of compression solutions based on different GS baseline models.

Table 1: Selected visual scenes specifications.

Visual scene	#Train. images	Resolution [px.]	Visual scene	#Train. images	Resolution [px.]
<i>africa</i>	56	1269×709	<i>garden</i>	161	1297×840
<i>basket</i>	74	1293×721	<i>kitchen</i>	244	1558×1039
<i>bicycle</i>	169	1237×822	<i>playroom</i>	196	1264×832
<i>bonsai</i>	255	1559×1039	<i>ship</i>	95	1266×711
<i>counter</i>	210	1558×1038	<i>train</i>	263	980×545
<i>drjohnson</i>	230	1332×876	<i>truck</i>	219	979×546
<i>flowers</i>	151	1256×828	—	—	—

4.1 Test Conditions

Each compression solution has one or more parameters to control the trade-off between model size (rate) and synthesis quality. For ContextGS, FCGS, and HAC++, this trade-off is explicitly controlled by a Lagrangian multiplier, λ , within the loss function. Compact3D and Reduced3DGS adjust the rate through VQ codebook sizes, with Reduced3DGS also using a Gaussian pruning level. SOG and GSICO-3DGS control compression through the JPEG XL quality level applied to the parameter images while GSICO-Scaffold-GS uses the quantization step size of the anchor and offset parameters. LightGaussian controls compression through Gaussian pruning percentages.

For each method, three operating points were defined: high quality (HQ), medium quality (MQ), and low quality (LQ), corresponding to progressively higher perceptual degradation (and lower rates). These operating points were determined through an expert pre-screening session, in which synthesized videos produced under several parameter settings were visually inspected for each method and scene, and the settings yielding the desired quality for each operating point were selected. The selected parameter settings for all scenes and compression solutions are provided on the dataset webpage. All GS models were trained and compressed on two NVIDIA GeForce RTX 4090 GPUs.

Across all compression solutions, scenes, and quality levels, a total of 331 stimuli were generated for subjective evaluation. This includes 26 reference sequences obtained by the two uncompressed baseline models for 13 scenes, and 305 test sequences corresponding to the compressed versions. While most methods were evaluated at the three quality levels across all 13 scenes, there are a few exceptions due to inherent limitations of some methods. FCGS was evaluated only at HQ, as its context model is exclusively trained for HQ compression. SOG was evaluated at HQ and MQ only, as even at its highest compression setting perceptual degradation was not very perceptible and scene geometry remained well-preserved. The same limitation was observed for GSICO-3DGS in 4 scenes (*counter*, *kitchen*, *flowers*, and *garden*). Finally, GSICO-Scaffold-GS does not provide an MQ level for the LF scenes, as quality degradation is abrupt when rate changes.

4.2 Subjective Methodology

The subjective assessment study follows the DSCQS methodology as defined in ITU-R BT.500 [26]. DSCQS is particularly suitable for GS compression evaluation because

participants rate both videos independently on a continuous scale, and without knowing which one is the reference. Moreover, this naturally accommodates cases where, due to compression, the test video is perceptually preferred over the uncompressed reference [27]. In each trial, participants are simultaneously shown the test and reference videos side-by-side, and rate each independently using a continuous slider with five quality levels, Bad, Poor, Fair, Good, and Excellent, corresponding to a scale from 1 to 5. The spatial position of the reference video and the presentation order of trials are randomized to minimize positional and contextual bias. Each video loops three times and participants can submit their scores only after the first playback.

To mitigate participant fatigue, the study is organized into three balanced test sessions, each covering a representative subset of compression solutions, scenes, and quality levels. For each scene, pairs of reference videos obtained from the two uncompressed baseline models were included, to enable score alignment and fair comparison between compression solutions using different baselines (cf. Section 5.2), allowing all DMOS values to be expressed on a common quality scale. The test is conducted on an ASUS ProArt PA32UC-K 4K HDR monitor at a spatial resolution of 1920×1080 pixels. To enable side-by-side presentation within the available screen space, each video is downsampled to a width of 940 pixels using bicubic interpolation, preserving the original aspect ratio.

Twenty non-expert observers participated in the study, 16 males and 4 females, aged between 18 and 35. Before the test, participants were informed of the test objective and completed a training session to familiarize themselves with the evaluation procedure and the range of expected visual distortions.

4.3 Data Processing

After data collection, outlier participants were identified using the kurtosis-based and correlation-based screening procedures recommended by ITU-R BT.500 [26], applied to the participants’ raw opinion scores, resulting in the exclusion of two participants by the second one; thus, $N = 18$ valid participants were retained. The opinion scores assigned to each pair of videos by each participant $p \in \{1, \dots, N\}$, for compression solution i with quality level l , against baseline model j and scene k , are denoted $OS_{\text{test}}^{(p,i,k,l)}$ and $OS_{\text{ref}}^{(p,j,k)}$, respectively. The differential opinion score (DOS) of a participant p for a given pair of videos is defined as:

$$\text{DOS}^{(p,i,j,k,l)} = OS_{\text{test}}^{(p,i,k,l)} - OS_{\text{ref}}^{(p,j,k)} \quad (1)$$

and the differential mean opinion score (DMOS) was obtained by averaging DOS across all valid participants:

$$\text{DMOS}^{(i,j,k,l)} = 5 + \frac{1}{N} \sum_{p=1}^N \text{DOS}^{(p,i,j,k,l)} \quad (2)$$

Under this formulation, higher DMOS values indicate higher perceived quality, preserving the intuitive interpretation of the MOS scale. Notably, DMOS values exceeding the nominal MOS range (i.e., 5) may occur when the test sequence was judged perceptually superior in quality to the baseline reference.

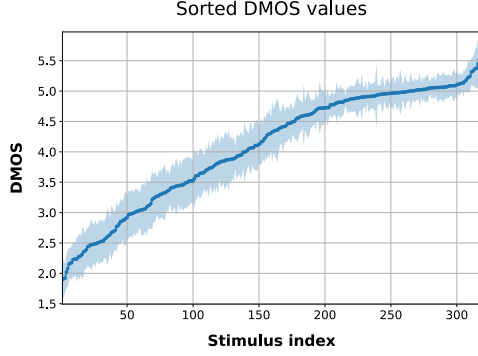


Figure 2: Sorted DMOS values with 95% confidence intervals.

When comparing compression solutions designed for different baseline models, the DMOS values computed using (2) are not directly comparable, as they are expressed relative to different references, namely videos synthesized from different uncompressed GS models. To enable a fair unified comparison, a reference compensation procedure is applied to adapt the DMOS of Scaffold-GS-based solutions relative to 3DGS, which was chosen as the common reference given it is the seminal GS model.

Reference compensation is performed using the direct comparison between the videos that resulted from the two uncompressed baseline models. For each participant p , Scaffold-GS-based compression solution i , scene k , and quality level l , the compensated DOS with respect to 3DGS as reference, is derived as:

$$\begin{aligned} \text{DOS}_{\text{comp}}^{(p,i,3\text{DGS},k,l)} &= \text{OS}_{\text{test}}^{(p,i,k,l)} - \text{OS}_{\text{ref}}^{(p,3\text{DGS},k)} \\ &= \left(\text{OS}_{\text{test}}^{(p,i,k,l)} - \text{OS}_{\text{ref}}^{(p,\text{SGS},k)} \right) - \left(\text{OS}_{\text{ref}}^{(p,3\text{DGS},k)} - \text{OS}_{\text{ref}}^{(p,\text{SGS},k)} \right) \quad (3) \\ &= \text{DOS}^{(p,i,\text{SGS},k,l)} - \text{DOS}^{(p,3\text{DGS},\text{SGS},k)} \end{aligned}$$

where $\text{OS}_{\text{ref}}^{(p,3\text{DGS},k)}$ and $\text{OS}_{\text{ref}}^{(p,\text{SGS},k)}$ are the participant's opinion score regarding the 3DGS and Scaffold-GS (or SGS) baseline models, respectively, $\text{DOS}^{(p,i,\text{SGS},k,l)}$ is the DOS between the Scaffold-GS-based compression solution and Scaffold-GS, and $\text{DOS}^{(p,3\text{DGS},\text{SGS},k)}$ is the DOS between the two baseline models. The other equation elements are as defined in (1). The compensated DMOS is then obtained by averaging the compensated DOS over all participants and adding an offset of 5. This procedure enables a unified RD comparison of all compression solutions regardless of their GS baseline model.

5 Experimental Results and Analysis

This section analyzes the subjective scores collected in the experiment and benchmarks the considered GS compression solutions. Section 5.1 presents and analyzes the DMOS scores, including a non-inferiority statistical test. Section 5.2 evaluates compression performance through perceptual RD analysis.

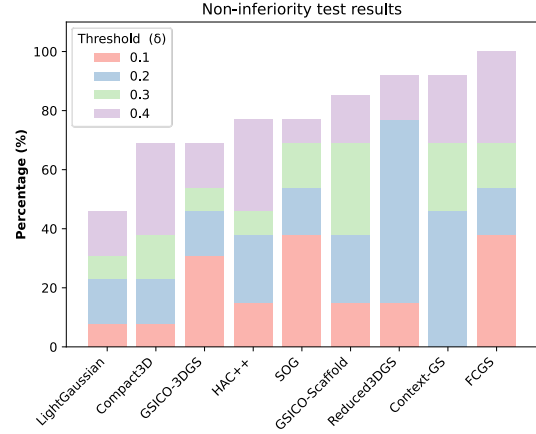


Figure 3: Non-inferiority statistical test results per GS compression solution.

5.1 Quality Assessment

Figure 2 presents the DMOS values of all tested stimuli, sorted in ascending order, together with their 95% confidence intervals (CI). The scores span a wide perceptual range, from low to high quality, confirming that the selected compression configurations provide a representative and diverse set of perceptual conditions. A Cronbach's alpha of 0.983 was obtained across all participant scores, indicating excellent inter-participant agreement and validating the reliability of the collected subjective data.

A significant number of stimuli exhibit DMOS values greater than 5, indicating that compressed versions are perceived as having higher quality than the uncompressed reference. This effect is particularly pronounced for joint training and compression solutions, where compression integrated into training acts as regularization, reducing noise and redundancy in the Gaussian representation. Methods such as ContextGS and HAC++ exploit spatial correlations through context modeling and structured representations, promoting consistency across neighboring Gaussians. This reduces geometric instability and enables more coherent rendering, especially in challenging regions. A similar, though less pronounced, effect occurs for post-training methods with Gaussian pruning, where removing redundant primitives improves visual quality despite compression.

To formally assess cases where compressed sequences are perceptually equivalent or superior to the uncompressed reference, a non-inferiority test is applied to HQ stimuli. The null hypothesis states that the quality of the compressed sequence is inferior to the reference by more than a predefined threshold δ . Rejection of the null hypothesis occurs when the lower bound of the 95% confidence interval of the difference between the mean opinion scores of the compressed and reference sequences exceeds $-\delta$, indicating that the compressed sequence is not perceptually worse than the reference beyond the accepted tolerance. In terms of DMOS, this is equivalent to requiring the lower bound of the 95% CI to exceed $5 - \delta$. The test was applied for $\delta \in \{0.1, 0.2, 0.3, 0.4\}$. Figure 3 shows, for each compression solution, the percentage of HQ stimuli for which the null hypothesis is rejected at each δ . Full statistical results are available on the

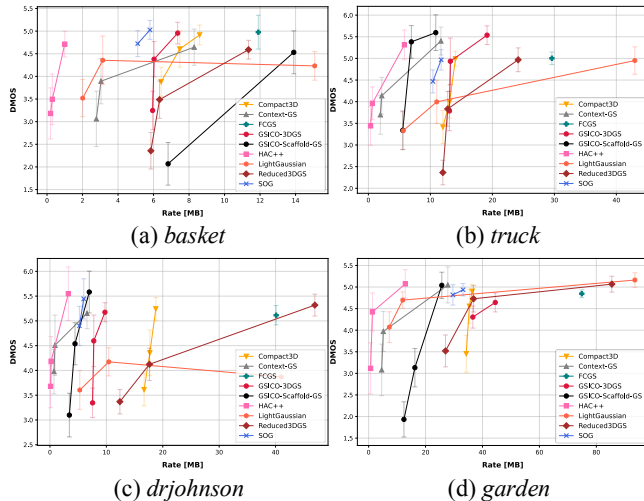


Figure 4: RD curves for benchmarking GS compression.

GScomp-QA dataset webpage. Figure 3 shows that most compression solutions are able to achieve perceptual quality levels equivalent to or better than the reference. In particular, joint training and compression solutions, such as Reduced3DGS and ContextGS, rank among the best-performing methods, with 92% of HQ compressed sequences generated by those methods not perceived as inferior to the reference at a threshold of 0.4.

5.2 GS Compression

RD performance is evaluated by defining the rate as the bitstream size in megabytes (MB) and the distortion as the average DMOS of each scene and quality level. Figure 4 depicts RD curves (with the respective DMOS CIs) for four representative scenes, one from each dataset. RD plots for the remaining scenes are provided in the dataset webpage [3]. For Scaffold-GS-based compression solutions, the compensated DMOS values are used. These results reveal clear trends across compression strategies. Joint training and compression solutions, particularly HAC++ and ContextGS, are the best at low rates. This stems from jointly optimizing representation and compression, allowing them to exploit strong spatial correlations and structural priors more effectively. In contrast, post-training methods exhibit lower compression efficiency, as they operate on fixed representations. Among post-training approaches, image-based approaches such as GSICD-Scaffold-GS and SOG achieve the best RD trade-offs, highlighting the effectiveness of leveraging mature 2D coding techniques for GS parameter compression. Finally, LightGaussian demonstrates the benefits of combining Gaussian pruning with model fine-tuning to jointly reduce model complexity and representation noise.

6 Objective Quality Metrics Benchmarking

This section evaluates how well existing objective quality metrics predict the perceptual impact of GS compression, using the GScomp-QA dataset. A broad set of full-reference metrics is considered, including classical solutions, namely FSIM [28], FVVD [29], GMSD [30], IW-SSIM [31], MAD [32], MSE-RGB,

Table 2: Correlation results of objective quality metrics.

Metric	PLCC	SROCC	Metric	PLCC	SROCC
MSE-RGB	0.593	0.621	VSI	0.726	0.713
PSNR-Y	0.610	0.611	MAD	0.735	0.726
PSNR-YUV	0.558	0.567	LPIPS	0.738	0.732
PSNR-HVS	0.729	0.716	ST-LPIPS	0.822	0.830
SSIM	0.646	0.636	DISTS	0.673	0.668
MS-SSIM	0.643	0.641	GMSD	0.825	0.823
IW-SSIM	0.796	0.778	NLPD	0.881	0.866
VIFp	0.791	0.778	VMAF	0.825	0.800
FSIM	0.830	0.816	FVVD	0.678	0.668

MS-SSIM [33], NLPD [34], PSNR-HVS [35], PSNR-Y, PSNR-YUV, SSIM [36], VIF [37], and VSI [38], as well as learning-based approaches, namely DISTS [39], LPIPS [40], ST-LPIPS [41], and VMAF [42]. The performance of each metric is assessed by measuring its correlation with subjective scores, using three standard criteria: the Pearson Linear Correlation Coefficient (PLCC), computed after cubic regression; Spearman Rank Order Correlation Coefficient (SROCC); Root Mean Squared Error (RMSE); and Perceptually Weighted Ranking Correlation (PWRC) [43]. Experimental results are summarized in Table 2. RMSE and PWRC results are presented in the dataset webpage [3], alongside a statistical significance analysis of the metrics' performances.

Overall, NLPD achieves the highest correlation across all criteria (with PLCC of 0.88 and SROCC of 0.87), followed by ST-LPIPS, FSIM, GMSD, and VMAF, reflecting the benefits of incorporating structural sensitivity and visual system modeling or adopting a learning-based approach. However, even the best-performing metrics fail to achieve near-perfect correlation. This limitation stems from the specific nature of GS compression artifacts, which differ from those in conventional image and video coding. In particular, GS compression introduces geometry-related distortions, view-dependent inconsistencies, and temporal instabilities that are not explicitly modeled by existing metrics. As a result, current metrics may not reliably guide the optimization of GS compression solutions, highlighting the need for specific quality metrics, and positioning GScomp-QA as a benchmark for their development and validation.

7 Conclusion

This paper proposes GScomp-QA, a subjective dataset for the quality assessment of compressed GS view synthesis, where compression-induced distortions are isolated from synthesis artifacts. Based on this dataset, a benchmark of recent GS compression solutions was conducted, showing that joint training and compression approaches achieve the best perceptual rate-distortion performance. A set of commonly used objective quality metrics was further evaluated, showing that while perceptually motivated metrics such as NLPD achieve higher correlation with subjective scores, existing metrics remain insufficient to fully capture GS-compression specific distortions. These results highlight the need for dedicated metrics capable of guiding the optimization and evaluation of GS compression solutions. GScomp-QA provides a resource to support this research direction.

REFERENCES

- [1] Ben Fei, Jingyi Xu, Rui Zhang, Qingyuan Zhou, Weidong Yang, and Ying He. 2025. 3D Gaussian Splatting as a New Era: A Survey. *IEEE Transactions on Visualization and Computer Graphics* 31, 8 (2025), 4429–4449.
- [2] Bernhard Kerbl, Georgios Kopanas, Thomas Leimkuehler, and George Drettakis. 2023. 3D Gaussian Splatting for Real-Time Radiance Field Rendering. *ACM Transactions on Graphics* 42, 4 (July 2023).
- [3] Link will be available after acceptance.
- [4] Pedro Martin, António Rodrigues, João Ascenso, and Maria Paula Queluz. 2025. GS-QA: Comprehensive Quality Assessment Benchmark for Gaussian Splatting View Synthesis. In *17th IEEE International Conference on Quality of Multimedia Experience (QoMEX)*, 1–7.
- [5] Yuke Xing, Jiarui Wang, Peizhi Niu, Wenjie Huang, Guangtao Zhai, and Yiling Xu. 2025. 3DGS-IEval-15K: A Large-scale Image Quality Evaluation Database for 3D Gaussian-Splatting. In *33rd ACM International Conference on Multimedia (MM)*, 12682–12689.
- [6] Yuke Xing, William Gordon, Qi Yang, Kaifa Yang, Jiarui Wang, and Yiling Xu. 2025. 3DGS-VBench: A Comprehensive Video Quality Evaluation Benchmark for 3DGS Compression. In *2025 IEEE International Conference on Visual Communications and Image Processing (VCIP)*, 1–5.
- [7] Zhaolin Wan, Yining Diao, Jingqi Xu, Hao Wang, Zhiyang Li, Xiaopeng Fan, Wangmeng Zuo, and Debin Zhao. 2026. Perceptual Quality Assessment of 3D Gaussian Splatting: A Subjective Dataset and Prediction Metric. In *AAAI Conference on Artificial Intelligence (AAAI)*, 40, 12, 9657–9665.
- [8] Tianang Chen, Jian Jin, Shilv Cai, Zhuangzi Li, and Weisi Lin. 2026. MUGSQA: Novel Multi-Uncertainty-Based Gaussian Splatting Quality Assessment Method, Dataset, and Benchmarks. *ArXiv:2511.06830* [cs.CV] <https://arxiv.org/abs/2511.06830>.
- [9] Qi Yang, Kaifa Yang, Yuke Xing, Yiling Xu, and Zhu Li. 2024. A Benchmark for Gaussian Splatting Compression and Quality Assessment Study. In *6th ACM International Conference on Multimedia in Asia (MMAsia)*, 12.
- [10] Johannes Lutz Schönberger and Jan-Michael Frahm. 2016. Structure-from-Motion Revisited. In *IEEE/CVF Conference on Computer Vision and Pattern Recognition (CVPR)*.
- [11] Johannes Lutz Schönberger, Enliang Zheng, Marc Pollefeys, and Jan-Michael Frahm. 2016. Pixelwise View Selection for Unstructured Multi-View Stereo. In *European Conference on Computer Vision (ECCV)*.
- [12] Tao Lu, Mulin Yu, Linning Xu, Yuanbo Xiangli, Limin Wang, Dahua Lin, and Bo Dai. 2024. Scaffold-GS: Structured 3D Gaussians for View-Adaptive Rendering. In *IEEE/CVF Conference on Computer Vision and Pattern Recognition (CVPR)*, 20654–20664.
- [13] Sharath Girish, Kamal Gupta, and Abhinav Shrivastava. 2024. Eagles: Efficient Accelerated 3D Gaussians with Lightweight Encodings. In *European Conference on Computer Vision (ECCV)*, 54–71.
- [14] Panagiotis Papantonakis, Georgios Kopanas, Bernhard Kerbl, Alexandre Lanvin, and George Drettakis. 2024. Reducing the Memory Footprint of 3D Gaussian Splatting. *ACM Computer Graphics and Interactive Techniques* 7, 1.
- [15] K. L. Navaneet, Kossar Pourahmadi Meibodi, Soroush Abbasi Koohpayegani, and Hamed Pirsiavash. 2023. Compact3D: Smaller and Faster Gaussian Splatting with Vector Quantization. *ArXiv:2311.18159* [cs.CV] <https://arxiv.org/abs/2311.18159>.
- [16] Yihang Chen, Qianyi Wu, Weiyao Lin, Mehrtash Harandi, and Jianfei Cai. 2025. HAC++: Towards 100X Compression of 3D Gaussian Splatting. *ArXiv:2501.12255* [cs.CV] <https://arxiv.org/abs/2501.12255>.
- [17] Yufei Wang, Zhihao Li, Lanqing Guo, Wenhan Yang, Alex C. Kot, and Bihan Wen. 2024. ContextGS: Compact 3D Gaussian Splatting with Anchor Level Context Model. *ArXiv:2405.20721* [cs.CV] <https://arxiv.org/abs/2405.20721>.
- [18] Pedro Martin, António Rodrigues, João Ascenso, and Maria Paula Queluz. 2026. Structured Image-based Coding for Efficient Gaussian Splatting Compression. *ArXiv:2601.14510* [cs.MM] <https://arxiv.org/abs/2601.14510>.
- [19] Yihang Chen, Qianyi Wu, Mengyao Li, Weiyao Lin, Mehrtash Harandi, and Jianfei Cai. 2025. Fast Feedforward 3D Gaussian Splatting Compression. *ArXiv:2410.08017* [cs.CV] <https://arxiv.org/abs/2410.08017>.
- [20] Wieland Morgenstern, Florian Barthel, Anna Hilsman, and Peter Eisert. 2025. Compact 3D Scene Representation via Self-Organizing Gaussian Grids. In *European Conference on Computer Vision (ECCV)*, Springer Nature Switzerland, Cham, 18–34.
- [21] Zhiwen Fan, Kevin Wang, Kairun Wen, Zehao Zhu, Debiao Xu, and Zhangyang Wang. 2024. LightGaussian: unbounded 3D Gaussian compression with 15× reduction and 200+ FPS. In *38th International Conference on Neural Information Processing Systems (NeurIPS)*. Vancouver, BC, Canada.
- [22] Arno Knapitsch, Jaesik Park, Qian-Yi Zhou, and Vladlen Koltun. 2017. Tanks and temples: Benchmarking large-scale scene reconstruction. *ACM Transactions on Graphics* 36, 4 (2017), 1–13.
- [23] Peter Hedman, Julien Philip, True Price, Jan-Michael Frahm, George Drettakis, and Gabriel Brostow. 2018. Deep blending for free-viewpoint image-based rendering. *ACM Transactions on Graphics* 37, 6 (2018), 1–15.
- [24] Kaan Yucer, Alexander Sorkine-Hornung, Oliver Wang, and Olga Sorkine-Hornung. 2016. Efficient 3D object segmentation from densely sampled light fields with applications to 3D reconstruction. *ACM Transactions on Graphics* 35, 3 (2016).
- [25] Jonathan T. Barron, Ben Mildenhall, Dor Verbin, Pratul P. Srinivasan, and Peter Hedman. 2022. Mip-NeRF 360: Unbounded Anti-Aliased Neural Radiance Fields. In *IEEE/CVF Conference on Computer Vision and Pattern Recognition (CVPR)*, 5470–5479.
- [26] ITU Recommendation BT. 2023. 500-15, Methodologies for the subjective assessment of the quality of television images. Geneva: International Telecommunication Union (2023).
- [27] Michael T. Bagdasarian, Philipp Knoll, Yifan Li, Florian Barthel, Andreas Hilsman, Peter Eisert, and Wolfgang Morgenstern. 2025. 3DGS.zip: A Survey on 3D Gaussian Splatting Compression Methods. *Computer Graphics Forum* 44, 2 (2025), e70078.
- [28] Lin Zhang, Lei Zhang, Xuanqin Mou, and David Zhang. 2011. FSIM: A Feature Similarity Index for Image Quality Assessment. *IEEE Transactions on Image Processing* 20, 8 (Aug. 2011), 2378–2386.
- [29] Rafal K. Mantiuk, Gyorgy Denes, Alexandre Chapiro, Anton Kaplanyan, Gizem Rufo, Romain Bachy, Trisha Lian, and Anjul Patney. 2021. FovVideoVDP: A Visible Difference Predictor for Wide Field-of-View Video. *ACM Transactions on Graphics* 40, 4 (Jul. 2021).
- [30] Bing Zhang, Pedro V. Sander, and Amine Bermak. 2017. Gradient Magnitude Similarity Deviation on Multiple Scales for Color Image Quality Assessment. In *IEEE International Conference on Acoustics, Speech and Signal Processing (ICASSP)*. New Orleans, LA, USA, 1253–1257.
- [31] Zhou Wang and Qiang Li. 2011. Information Content Weighting for Perceptual Image Quality Assessment. *IEEE Transactions on Image Processing* 20, 5 (May 2011), 1185–1198.
- [32] Eric C. Larson and Damon M. Chandler. 2010. Most Apparent Distortion: Full-Reference Image Quality Assessment and the Role of Strategy. *Journal of Electronic Imaging* 19, 1 (Jan. 2010), 011006.
- [33] Zhou Wang, Eero P. Simoncelli, and Alan C. Bovik. 2003. Multiscale Structural Similarity for Image Quality Assessment. In *IEEE Asilomar Conference on Signals, Systems, and Computers (ACSSC)*. Pacific Grove, CA, USA, 1398–1402.
- [34] Valero Laparra, Alexander Berardino, Johannes Ballé, and Eero P. Simoncelli. 2017. Perceptually Optimized Image Rendering. *Journal of the Optical Society of America A* 34, 9 (Sep. 2017), 1511–1525.
- [35] Prabhjot Kaur Gupta, Priti Srivastava, Shefali Bhardwaj, and Vikrant Bhatnagar. 2011. A Modified PSNR Metric Based on HVS for Quality Assessment of Color Images. In *IEEE International Conference Communication and Industrial Application (ICCIA)*. IEEE, Kolkata, India, 1–4.
- [36] Zhou Wang, Alan C. Bovik, Hamid R. Sheikh, and Eero P. Simoncelli. 2004. Image Quality Assessment: From Error Visibility to Structural Similarity. *IEEE Transactions on Image Processing* 13, 4 (Apr. 2004), 600–612.
- [37] Hamid R. Sheikh and Alan C. Bovik. 2006. Image Information and Visual Quality. *IEEE Transactions on Image Processing* 15, 2 (Feb. 2006), 430–444.
- [38] Lin Zhang, Ying Shen, and Hongyu Li. 2014. VSI: A Visual Saliency-Induced Index for Perceptual Image Quality Assessment. *IEEE Transactions on Image Processing* 23, 10 (Oct. 2014), 4270–4281.
- [39] Keyan Ding, Kede Ma, Shiqi Wang, and Eero P. Simoncelli. 2022. Image Quality Assessment: Unifying Structure and Texture Similarity. *IEEE Transactions on Pattern Analysis and Machine Intelligence* 44, 5 (May 2022), 2567–2581.
- [40] Richard Zhang, Phillip Isola, Alexei A. Efros, Eli Shechtman, and Oliver Wang. 2018. The Unreasonable Effectiveness of Deep Features as a Perceptual Metric. In *IEEE/CVF Conference on Computer Vision and Pattern Recognition (CVPR)*. Salt Lake City, UT, USA, 586–595.
- [41] Abhijay Ghildyal and Feng Liu. 2022. Shift-Tolerant Perceptual Similarity Metric. In *European Conference on Computer Vision (ECCV)*. Springer, Berlin, Heidelberg, 91–107.
- [42] Zhi Li, Aaron Aaron, Ioannis Katsavounidis, Anush Moorthy, and Megha Manohara. 2017. Toward a Practical Perceptual Video Quality Metric. *Medium* (Apr. 2017).
- [43] Qingbo Wu, Hongliang Li, Fanman Meng, and King N. Ngan. 2018. A Perceptually Weighted Rank Correlation Indicator for Objective Image Quality Assessment. *IEEE Transactions on Image Processing* 27, 5 (2018), 2499–2513.